Journal of Power Sources 180 (2008) 890–895

Contents lists available at ScienceDirect

Journal of Power Sources

journal homepage: www.elsevier.com/locate/jpowsour

Short communication

Influence of chemical modification of activated carbon surface on characteristics of supercapacitors

B.P. Bakhmatyuk[a,*], B.Ya. Venhryn[a], I.I. Grygorchak[a], M.M. Micov[b]

[a] Lviv Polytechnic National University, 12 St. Bandera Street, Lviv 79013, Ukraine
[b] Concern "Hefra", 133 Podhaj Street, Bratislava 84103, Slovak Republic

ARTICLE INFO

Article history:
Received 20 November 2007
Received in revised form 25 January 2008
Accepted 17 February 2008
Available online 26 February 2008

Keywords:
Modified activated carbon
Electrochemical impedance spectroscopy
Supercapacitor
X-ray photoelectron spectroscopy
Specific capacitance
Specific energy

ABSTRACT

The influence of the change of Fermi level electrons position of activated carbon μ_C caused by chemical modification of its porous surface by Mn^{2+} ions on its capacitive characteristics in 7.6 m KOH, 4 m KI, 2 m ZnI_2 aqueous solutions is investigated in this work. The detection of adsorbed Mn^{2+} ions on the surface of activated carbon was carried out according to methods of secondary ionic mass spectrometry (SIMS). An increase in electronic density on the Fermi level of modified with Mn^{2+} activated carbon was determined with a help of X-ray photoelectron spectroscopy (XPS) data. Capacitive characteristics of the electrodes have been investigated by means of electrochemical impedance spectroscopy, computer modeling, and galvanic discharge. The correlation between electronic structure of modified activated carbon (MAC) and thermodynamic characteristics of ions of the used electrolytes is established. On the basic of the obtained experimental data, electrochemical system of the hybrid capacitor with a specific capacitance of 1740 F g^{-1} and with a specific energy of 30 mWh g^{-1} is developed.

1. Introduction

The main advantages of supercapacitors over batteries are their specific power which is many times greater and their number of charge–discharge cycles. But they are considerably inferior in their specific energy which, according to [1], makes up less than 10%. As to the nature of the used capacity, supercapacitors, as it was shown in [2], can be conventionally divided into the two types: (a) capacitors working at the expense of charge–discharge of their electric double layers (EDL) of the blocking electrode–electrolyte interface; they are called electric double-layer capacitors (EDLC) and (b) pseudocapacitors working due well reversible electroadsorption of ions from the electrolyte or at the expense of surface redox reactions. The application of different carbonations materials with large specific surface (of 1000–3000 m^2 g^{-1}) enables us to develop EDLC with capacitance of several tens Farads per a gram of electrode material. In [1], it was reported about continuous process of inventing new materials which can ensure the increase in specific capacitance of supercapacitors up to 900 F g^{-1}, for example, carbonaceous nanotubes with set diameter of pores and specific surface; ruthenium oxide which is able to volumetrically introduce a proton, and manganese dioxide. In [3] the value of the specific capacitance of 1156 F g^{-1} for intercalatiously modified TiS_2 in 1 M $LiBF_4$ in γ-butyrolactone is achieved, and in [4], the possibility of obtaining a specific capacitance of 2000 F g^{-1} for electroadsorption of I^- into pores of $d \lesssim 4.4$ Å of activated carbon with a total area 1000 m^2 g^{-1} according to intercalation mechanism is shown. In [1], the achievement of energy density up to 88.5 Wh kg^{-1} for capacitors of carbonaceous materials able to chemically intercalate ions is foreseen. In [5–9], the influence of the capacitance of a region of spatial charge of carbonations material on the capacitance of double electric layer of its interface with electrolyte is investigated. The dependences of state densities on Fermi level shift (in scale of electron potentials) which have their minimum at zero charge potential [10] have been plotted. We have investigated the influence of electronic properties of activated carbonaceous material (AC) obtained by means of high temperature carbonization of synthetic materials and fruit stones on its capacitive characteristics in 7.6 m KOH and 4 m KI aqueous solutions. The agreement of electronic properties of AC with thermodynamic parameters of electrolyte ions enables us to obtain reversive pseudocapacitance of 2000 F g^{-1} in 4 m KI solution. In particular, the impossibility to obtain large values of pseudocapacitance for the materials with $\mu_C \leq -4.3$ eV under these conditions is shown; for example, for AC obtained from fruit stones. The idea of forethought increase in the filling of electron states valence band of activated carbon through doping is connected with in EDL capacitance. In [11], it is shown that 3d-transition metals and rare earth elements possess the greatest density of electron states

* Corresponding author. Tel.: +380 322582267.
E-mail addresses: bgbakhm@rambler.ru (B.P. Bakhmatyuk), venhryn_b@ukr.net (B.Ya. Venhryn), ivangr@rambler.ru (I.I. Grygorchak), miron@mail.lviv.ua (M.M. Micov).

0378-7753/$ – see front matter © 2008 Published by Elsevier B.V.
doi:10.1016/j.jpowsour.2008.02.045

near Fermi level. And in [12] chemical composite of Mn_3O_4 with carbon which possess high electronic conductance and high pseudocapacitance that makes it a prospective material for electrodes of supercapacitors is investigated. To study the influence of chemical modification of material surface (investigated in [4]) by Mn^{2+} ions on capacitive characteristics of materials in aqueous solutions of electrolytes is the aim of this work.

2. Experimental

Activated carbon obtained by means of activational carbonization of fruit stones and chemically modified by Mn^{2+} ions was used for our experiments. Its porous structure was investigated by methods of precision porometry and small angle X-ray scattering [13] with the use of ASAP 2000 M porometer and DRON-3 diffractometer, respectively. The detection of adsorbed Mn^{2+} ions on the surface of activated carbon was carried out according to SIMS methods with a help of MC-7201 mass-spectrometer. The used SIMS method is of the following technical data: Penning type ionic source which ensures primary ionic current of Ar^+ ions with the energy of 3–5 keV and a density of $\approx 5\ \mu A\ mm^{-2}$. The diameter of an etching stain is of 1–3 mm. The angle between primary electrons bombardment direction and the normal is 45°. The pressure residual gases in the object chamber is 7×10^5-8×10^5 Pa. The analysis of mass spectra is reduced to recording mass-spectral signal from secondary ions as a function of the time of sputtering. An increase in electronic density on the Fermi level of modified with Mn^{2+} activated carbon was determined with a help of X-ray photoelectron spectroscopy (XPS) data. As a method of chemical analysis, XPS ensures relative sensitivity of about 1%, absolute sensitivity of 10^{-6} to 10^{-8} g, and an accuracy of 5–10%. Electrochemical measurements were taken at room temperature according to two-electrode circuit with the reference electrode made of Zn and the counter electrode in the same electrolyte solution. All the electrode potentials given in the tables have been evaluated relative to standard hydrogen electrode. Energetic levels are given in absolute scale of energies. Galvanostatic and impedance (in the frequency range of 10^{-3} to 10^{-5} Hz) dependencies have been determined with a help of AUTOLAB measuring complex made in Netherlands by "ECO CHEMIE" in combination with FRA-2 and GPES computer programs. Impedance data have been modeled to equivalent electric circuit (EEC) with a help of ZView2 computer program. Values of capacitances for plotting the capacitance dependences have been determined from impedance measurements according to the formula: $C = (2\pi fImZ)^{-1}$ at the frequency of 1.0×10^{-3} Hz with the accuracy of 2–8% (Kramers–Kronig's test was within 10^{-6} to 10^{-5}) and at room temperature. 7.6 m KOH, 4 m KI, 2 m ZnI_2 aqueous solutions were used as electrolytes. 2 cm^2 working area electrodes in a nickel or steel net with 5% binder poly(vinyliden fluoride-*co*-hexafluoropropylene) have been fabricated for measurements. For our investigations, aqueous solutions of the electrolytes were sufficiently concentrated to ensure large capacitances of diffusive layer of electrolyte (Gouy–Chapman layer) >100 $\mu F\ cm^{-2}$ and also to ensure sufficient electric conductivity. Potentials of separation and chemical potentials of ions have been calculated according to the known from [14] formulas:

$$E = E_0 + \frac{RT}{nF} \ln\left(\frac{a_{oxid}}{a_{red}}\right), \quad (1)$$

$$\mu_s = \mu + RT \ln a_s, \quad (2)$$

here a_{oxid}, a_{red} and a_s are activities of ions in a solution.

Chemical modification of AC materials surface by Mn^{2+} ions was being carried out in a mixture of aqueous solutions of 5% $KMnO_4$, 5% nitric acid with 6% ethyl alcohol added at a temperature of 80 °C, and the mixture was being magnetically stirred for 8 h. The mass of FS activated carbon in the mixture amounted to 99.4 g per 0.6 g of Mn. Precipitate was filtered, washed with distillated water, dried at 150 °C for 8 h.

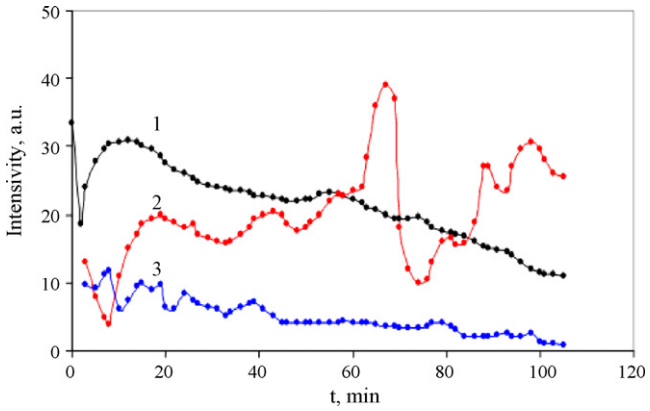

Fig. 1. Distribution of the elements C (curve 1), O (curve 2), Mn (curve 3) with respect to depth of specimen is given as a function of time of etching.

3. Results and discussions

In the course of chemical processing of AC by Mn^{2+} ions, the process of chemical reduction according to the scheme $Mn^{7+} + 5e^- \rightarrow Mn^{2+}$ took place. In Fig. 1, the distribution of the elements C (curve 1), O (curve 2), Mn (curve 3) with respect to depth of specimen is given as a function of time of etching; where t is the time of etching in minutes for 0.6% Mn^{2+} counted by mass. Arbitrary unit (a.u.) is the intensity of signal which we fix relative to a certain element. Normalization of mass-spectra with respect to phone mass-lines, intensity of which in first approximation may serve as a reference signal, shows that the intensity Mn in the case of drying after carrying out modification process at $T = 423$ K is 2.5 times higher as compared to the specimen the temperature of drying of which was $T = 373$ K.

In Fig. 2a, the spectrum of the valence band of non-modified activated carbon is shown; from this, it can be seen that it is of two-humped structure with considerable decrease of intensity when the binding energy approaches Fermi level. As it is seen from Fig. 2a, on Fermi level, this intensity $I(E_F)$ is proportional to electron density and equals 27,200.

After modification with Mn^{2+} ions, the form of the valence band essentially changes (Fig. 2b). It becomes practically one-humped with considerable increase in intensity $I(E_F)$ on Fermi level which equals 42,600. In this process, ions Mn^{2+} are being specifically absorbed on AC surface, these ions remain electrochemically non-active in the investigated range of potentials from −0.86 to 0.45 V because the standard electrode potential of the reaction of $Mn^{2+} + 2e \rightarrow Mn$ equals −1.179 V. Chemical modification of AC material surface by Mn^{2+} ions leads to the change in Fermi level

Table 1
Porometric and thermodynamic characteristics of investigated carbonaceous materials

Material	FS
Area of the pores ($m^2\ g^{-1}$)	
$d \lesssim 4.4$ Å	448
$4.4 < d < 19$ Å	498
$d > 19$ Å	181
Value of electrochemical potential (μ_F) (eV)	−4.16
Value of stationary potential in 4 m KI (E_{st}) (V)	0.32
Value of stationary potential in 7.6 m KOH (E_{st}) (V)	−0.15

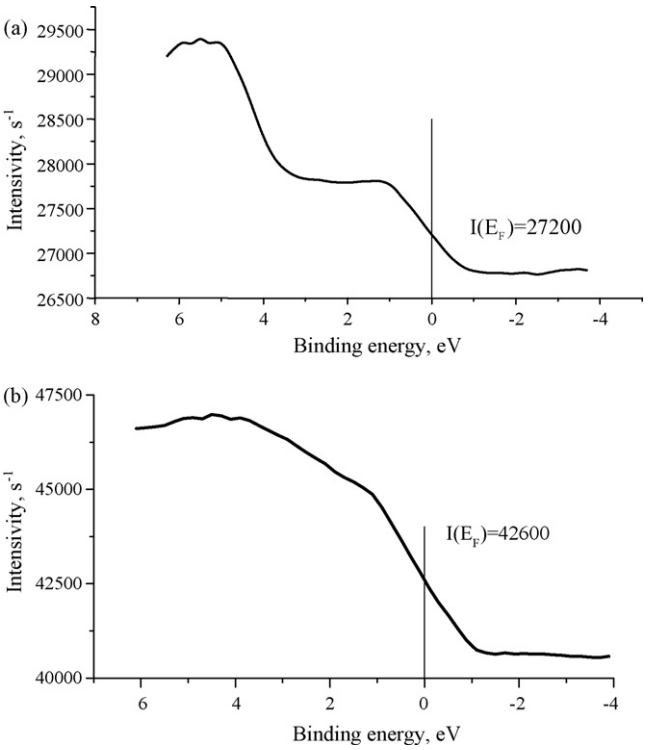

Fig. 2. XPS spectrum for AC (a) and MAC (b).

Table 2
Parameters of EEC (Fig. 4a)

k (number of chain)	R (Ω)	C (F)
1	0.29	2.8×10^{-5}
2	0.7	7.1×10^{-3}
3	0.21	0.09
4	0.91	0.37
5	8.87	0.27

position of the initial material from −4.3 to −4.16 eV (Table 1) without transformation of the porous structure of the material.

In a frequency range of 10^{-3}–268 Hz, Nyquist's plots of MAC electrodes in 7.6 m KOH solution are typical of double electric layer charge (Fig. 3a, curve 2) [15] and satisfactorily correspond to de Levie transmissional model for a porous electrode (Fig. 3a, curve 1) [16,17]. With this, the shift angle of phases equals −80° at 10^{-3} Hz (Fig. 3b). According to the linear de Levie model, the frequency dispersion of impedance can be expressed by the equation [18]:

$$Z(j\omega) = \left(\frac{R_D}{j\omega C_D}\right)^{1/2} \coth(j\omega R_D C_D)^{1/2}, \quad (3)$$

here R_D and C_D are the general distributive resistance and capacitance, respectively. R_D and C_D values calculated according to numerical parameters of EEC (Table 2) for MAC in 7.6 m KOH at −0.15 V are equal to 0.06 Ω cm^{-2} and 81.9 F g^{-1} (7.3 μF cm^{-2}), respectively. In a high frequency range of 268–10^4 Hz (Fig. 3a), a fragment of Faraday's loop which is modeled by parallel-connected capacitor and resistor is observed (Fig. 4b). This, for example in [19], is often caused by a passive film on carbonaceous materi-

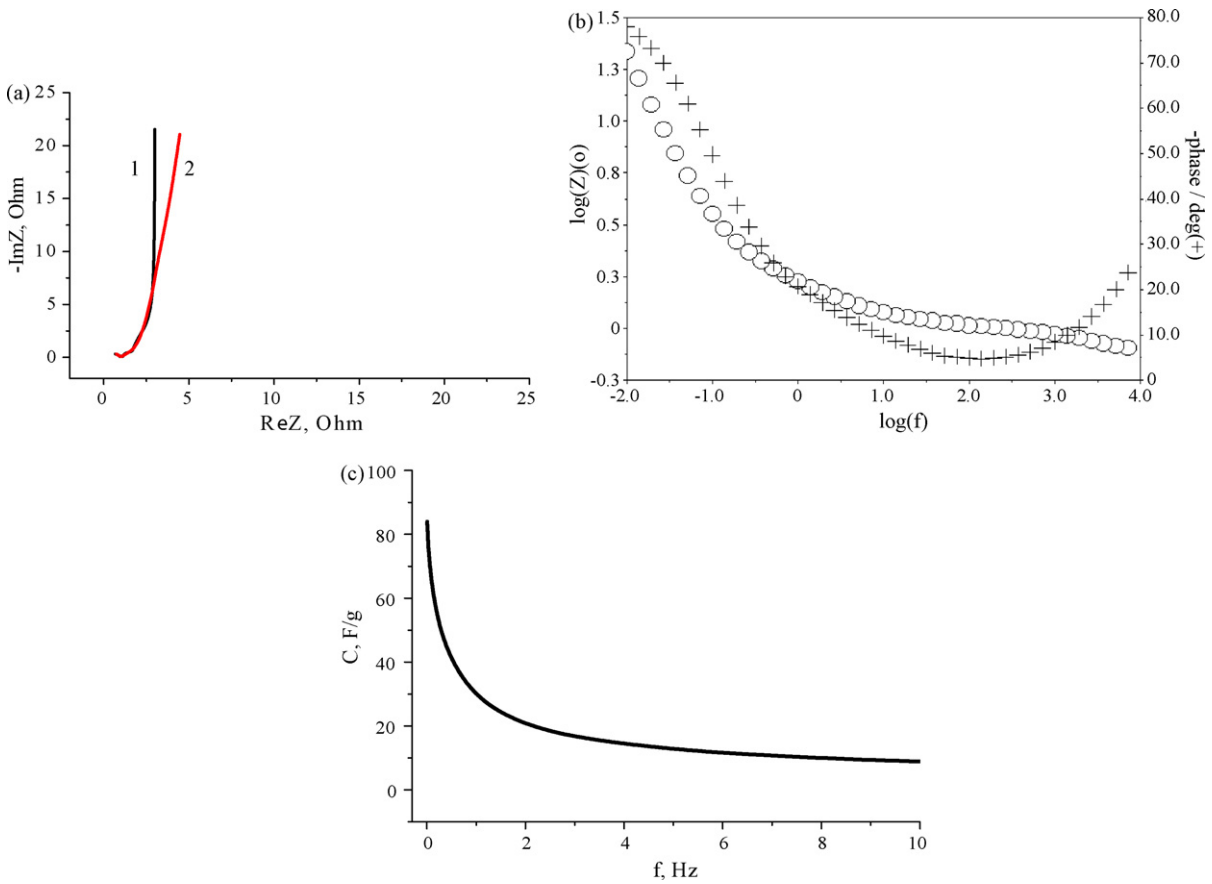

Fig. 3. Typical dependences: (a) impedance: (1) according to model; (2) experimental; (b) Bode dependence; (c) frequential dependence of capacitance for MAC in 7.6 m KOH at E_{st} = −0.15 V.

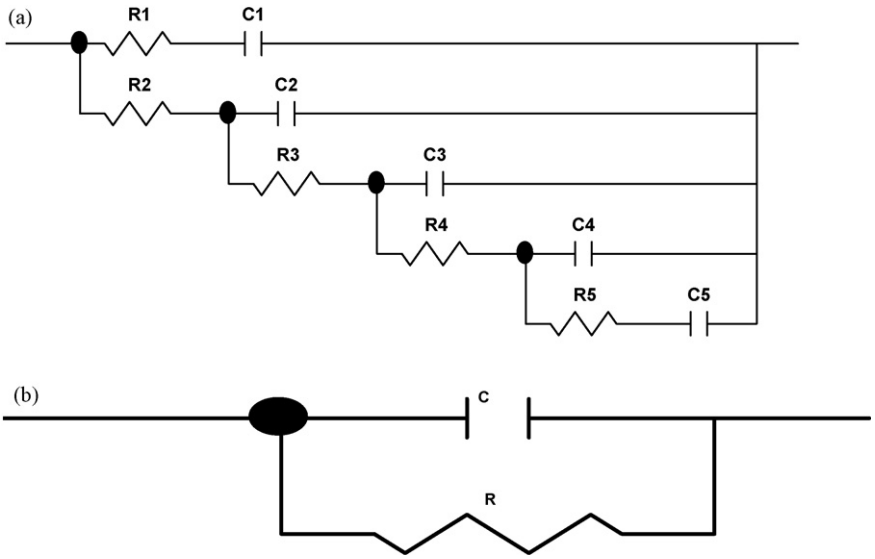

Fig. 4. Typical linear transmissional EEC of (a) interface between MAC and 7.6 m KOH at $E = -0.67$ V and (b) general parallel circuit of the same interface.

Table 3
Thermodynamic parameters of ions in different electrolyte solutions

Ion (solution)	Potential of ion separation (with reference to standard hydrogen electrode), V (eV)	Chemical potential of ion in solution (μ_{el}) (eV)	Free energy of ion hydration (according to Born) (eV)
K^+ (7.6 m KOH)	−2.84	−1.55	−5.35
I^- (2 m ZnI_2)	0.506 (−5.06)	−3.9	−3.3
Zn^{2+} (2 m ZnI_2)	−0.73	−3.67	−22.08 [20]
I^- (4 m KI)	0.511 (−5.011)	−3.89	−3.3
OH^- (7.6 m KOH)	0.32	−2.85	−4.9 to −5.0 [21,22]

als. Its resistance is identified with the migration resistance R_{mig} the value of which is 0.99 Ω cm^2 in our case. The value of specific capacitance of 83 F g^{-1} (Fig. 3c) gives no reason to assert that the contribution of pseudocapacity is an essential one. Sharp drop in AC capacitance with its positive polarization, in spite of the fact that the hydration of OH^--ion is somewhat less than that for K^+-ion (Table 3), is retained for MAC as well (Fig. 5a). This takes place due to sharp expansion of a spatial charge region (SChR) of carbonaceous material according to the equation [23]:

$$C_{SC}^{-2} = \frac{2L_D^2}{(\varepsilon_0\varepsilon_{SC})^2(|e\varphi_{SC}/kT| - 1)}, \quad (4)$$

here L_D is Debye width, ε_0 and ε_{SC} are dielectric constants, C_{SC} and φ_{SC} are the capacitance and electric potential of SChR, respectively. The expansion of SChR of electrode material leads to shunting of the dense part of double electric layer (Helmholtz layer) by its capacity that enables us to use this region (Mott–Schottky layer) for experimental determination of μ_C according to the known technique [23]. The intersection of the Mott–Schottky line at $C^{-2} = 0$ with the axis of potentials gives us the position of Fermi level in the scale of electrode potentials which in our case (Fig. 5b) equals −0.34 V (−4.16 eV). The essence of this technique and its application to our case has been considered in [4]. The change in μ_C by −0.14 eV leads (according to data obtained in [7,8]) to the increase in the density of states $D(\mu_F)$ at Fermi level that causes the increase in negative polarization of the electrode in 7.6 m KOH up to −0.87 V (Fig. 5a) and therefore also to the increase in maximal capacitance of the electrode to 170 F g^{-1} (Fig. 5a) as compared to the maximal charge of 82 F g^{-1} at −0.69 V for the initial material. The value $\mu_C = -4.16$ eV of MAC becomes sufficient for critical electrode potential $\varphi_{cr} = 0.28$ V according to the expression:

$$\varphi = \frac{\mu_{I^-} - \mu_C}{e} \quad (5)$$

for realization of the electrosorption of I^--ions from 4 m KI according to the scheme [24]:

$$A^-(mG) + C \leftrightarrow CA^{(1-\delta)-} + \delta e^-(inC) + (m-n)G, \quad (6)$$

here m and n are the numbers of hydration ion in solution and in sorbtive state, respectively; C is the positively charged carbonatious material.

Comparing the value $\varphi_{cr} = 0.28$ V with the experimentally obtained $E_{st} = 0.32$ V, the conclusion of the possibility of realization of the process of electrosorption of I^--ions according to the expression 6 can be drawn (in this case, without applying external polarization). Anode polarization of MAC from 0.32 to 0.45 V gives the increase in capacitance from 276 F g^{-1} (24.5 μF cm^{-2}) to 2307 F g^{-1} (205 μF cm^{-2}), Fig. 6. Such capacitance (>250 F g^{-1}) [16] is not typical EDL charge without an essential contribution of pseudocapacity [19].

Impedance dependencies of MAC (Figs. 7a and 8a) have a pronounced Faraday's loop in the frequency range of 0.28–2 × 10^3 Hz and (Fig. 7a) 286–2 × 10^3 Hz (Fig. 8a). It is conditioned by pseudocapacitive MAC charge by I^--ions the charge is described by the EEC (Fig. 4b) and by intercalation mechanism in accordance with theory of [4]. Determined (by the projection of Faraday's loop on abscissa axis) intercalation resistance R_{int} decreases from 17.96 to 12.94 Ω cm^2 under the anode polarization of 0.32–0.45 V. This is well accounted for by the ability of I^--ions to dehydrate due to their small dehydration energy (Table 1). The decrease in phase shift angle in 4 m KI, in comparison with that in 7.6 m KOH, from

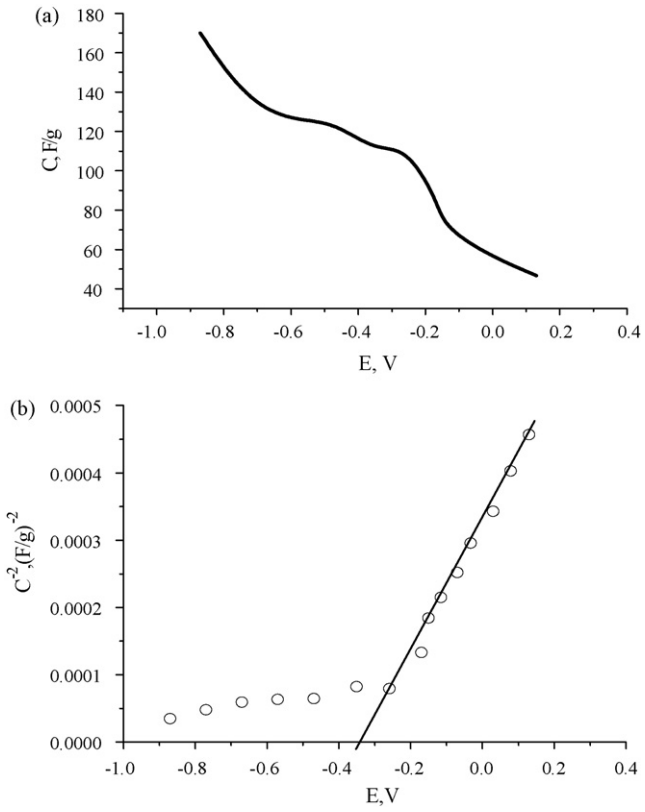

Fig. 5. Dependencies of capacitance (a) and inverse square of capacitance (b) of MAC electrode on electrode potential in 7.6 m KOH.

−80° to −60° (Figs. 3b and 7b) and −25° (Fig. 8b) serves an evidence of the increase in pseudocapacitive contribution into the electrode charge. Attention should be paid that the impedance data in low frequency ranges of 0.0015–0.25 Hz at 0.32 V (Fig. 7a) satisfactorily correspond to EEC (Fig. 4a) with the definite parameters $R_D = 29\ \Omega\,cm^2$ and $C_D = 309\ F\,g^{-1}$ ($27.4\ \mu F\,cm^{-2}$) and also to the transmission model of porous electrode possessing Faraday's capacitance in the frequency range of 0.0015–268 Hz at 0.42 and 0.45 V (Fig. 8) [14,15].

The possibility of the practical use of large intercalational pseudocapacity of iodine ions of MAC porous structures has been investigated in 2 m ZnI_2 with the counter electrode made of Zn and

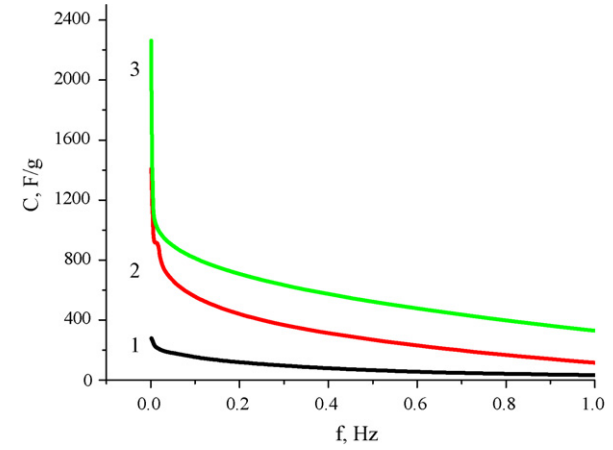

Fig. 6. Frequential dependencies of capacitance on frequency for MAC in 4 m KI at 0.32 V (1), 0.42 V (2) and 0.45 V (3).

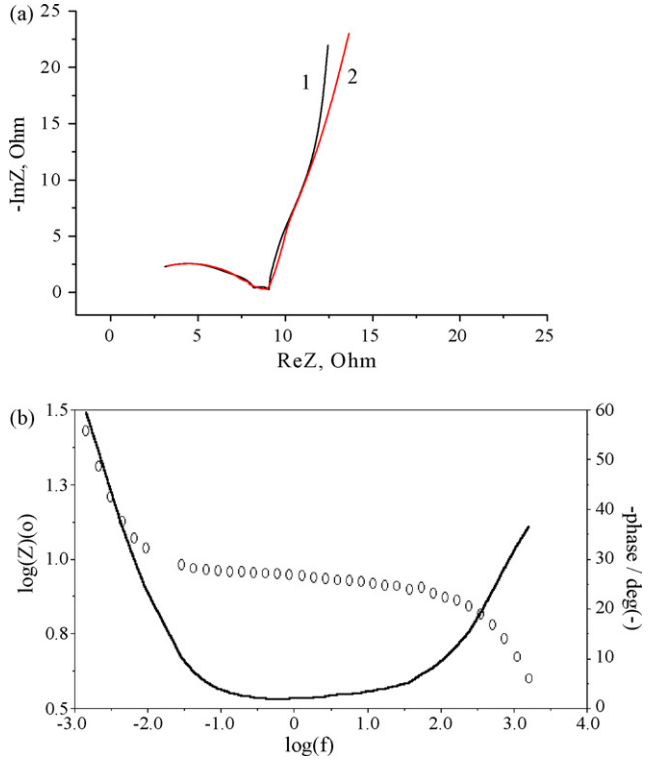

Fig. 7. Impedance dependences (a): (1) according to EEC (Fig. 4a); (2) experimental; Bode dependence (b) for MAC in 4 m KI at 0.32 V.

the reference electrode. The following scheme whose open circuit voltage $E_{oc} = 1.08$ V was used in our measuring:

$$Zn|2\ m\ ZnI_2|MAC. \quad (7)$$

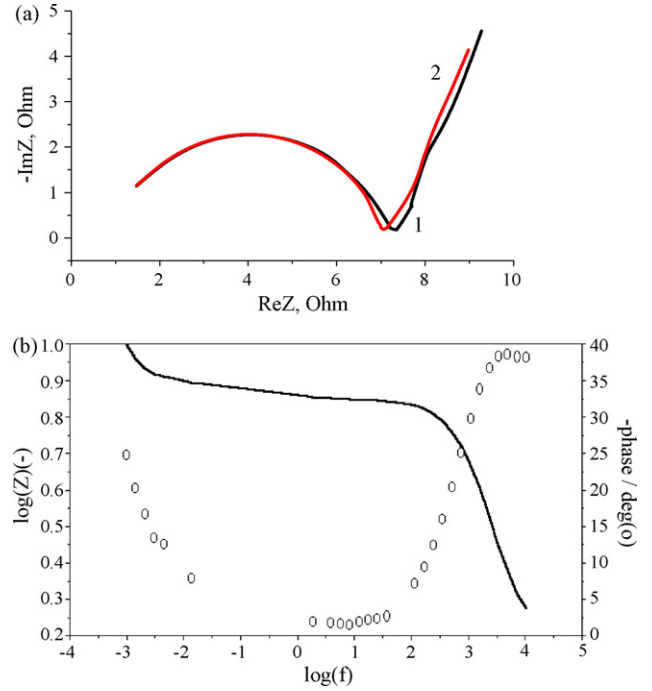

Fig. 8. Impedance (a) dependences at (1) 0.42 V; (2) 0.45 V and Bode dependence (b) at 0.42 V for MAC in 4 m KI.

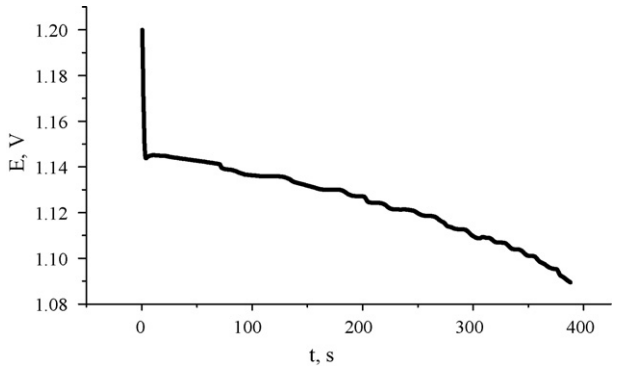

Fig. 9. Galvanostatic discharge ($i = 0.25\,A\,g^{-1}$) of MAC in 2 m ZnI_2 charged under potentiostatic conditions (at 1.2 V).

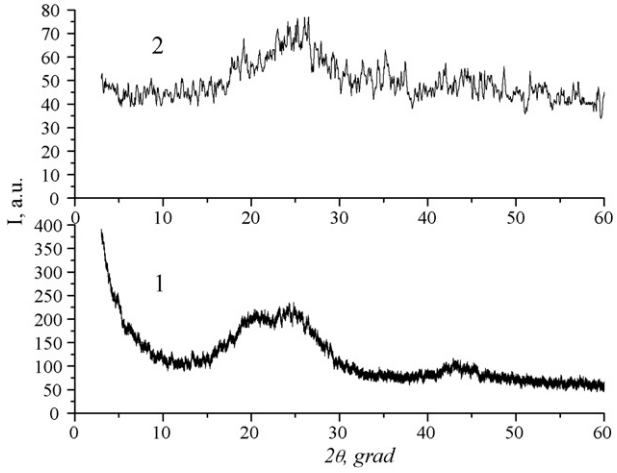

Fig. 10. Curves of X-ray scattering intensity for non-charged (1) and charged (2) MAC.

Taking into account the thermodynamic parameters of Zn electrode and 2 m ZnI_2 (Table 2), the necessary for the realization of the process of iodine adsorption in the given system according to expression 5 values $E_{st} = 0.3$ V and $\varphi_{cr} = 0.27$ V are determined. To charge the electrode, anode polarization under potentiostatic conditions at 1.2 V was applied. Galvanostatic discharge of the charged MAC of active mass $m_a = 0.012$ g with the current $I = 3 \times 10^{-3}$ A (Fig. 9) takes place at average discharge voltage of 1.13 V and ensures the discharge capacitance of 1740 F g^{-1} (26.6 mAh g^{-1}). The latter is calculated as follows:

$$C = \frac{I\,\Delta t}{\Delta E\, m_a} = \frac{3 \times 10^{-3}\,A \times 382.86c}{0.055\,V \times 0.012\,g} = 1740\,F\,g^{-1}. \quad (8)$$

As the result, specific energy amounts to 1.13 V × 26.6 mAh g^{-1} = 30 mWh g^{-1}.

X-ray scattering curves obtained in Cu Kα radiation (1.5418 Å) for activated carbon are given in Fig. 10. Essential increase in intensity in the range of small angles scattering (3–10°) observed in curve 1 for non-charged porous structure MAC. In the course of intercalation with iodine (curve 2), essential decrease in the intensity in the range of small angles of scattering, is observed, that is caused by processes of micropores filling. The location of the main maximum is practically unchanged, whereas its intensity essentially decreases. Considerable structural changes in the course of intercalation of MAC with iodine are not observed. However, there are essential changes of its porous structure, this indicates the filling of micropores with iodine ions in the course of the intercalation.

4. Conclusion

It is shown that the chemical modification of AC surface by Mn^{2+} ions leads to a shift in Fermi level location of the material to the negative side (scale of negative potentials) by 0.14 V and considerable increase in intensity $I(E_F)$ on Fermi level. This gives us a possibility to increase maximal capacitance of MAC in 7.6 m KOH more than twice at the expense of the increase in the density of states at the Fermi level. And what is more, the shift in Fermi level of MAC gives a possibility to achieve the values $\varphi_{cr} = 0.28$ V in 4 m KI and $\varphi_{cr} = 0.29$ V in 2 m ZnI_2 for the realization of electrosorption process of iodine and for ensuring anode polarization of 0.13 V for a charging of the electrode up to 2307 F g^{-1}. A hybride system which ensures the discharge capacitance of 1740 F g^{-1} and the specific energy of 30 mWh g^{-1} at an average discharge voltage of 1.13 V under galvanic conditions of the discharge with the current density of 0.25 A g^{-1} is developed.

References

[1] J.P. Zheng, Proceedings of the 14th International Seminar on Double Layer Capacitors and Hybrid Energy Storage Devices, Deerfield Beach, USA, 2004, p. 142.
[2] A.K. Shukla, S. Sampath, K. Vijayamohanan, Curr. Sci. 79 (2000) 1656.
[3] I.I. Grigorchak, Electrohimiya 39 (2003) 770.
[4] B.P. Bakhmatyuk, B.Ya. Venhryn, I.I. Grygorchak, M.M. Micov, Yu.O. Kulyk, Electrochim. Acta 52 (2007) 6604.
[5] M. Hahn, M. Baertschi, O. Barbieri, J.-C. Sauter, R. Kötz, R. Gallay, Electrochem. Solid-State Lett. 7 (2004) A33.
[6] J.P. Randin, E. Yeager, J. Electrochem. Soc. 118 (1971) 711.
[7] J.P. Randin, E. Yeager, J. Electroanal. Chem. 36 (1972) 257.
[8] H. Gerischer, J. Phys. Chem. 89 (1985) 4249.
[9] H. Gerischer, R. McIntyre, D. Scherson, W. Storck, J. Phys. Chem. 91 (1987) 1930.
[10] R. Kötz, M. Hahn, O. Barbieri, J.-C. Sauter, R. Gallay, Proceedings of the 13th International Seminar on Double Layer Capacitors and Hybrid Energy Storage Devices, Deerfield Beach, USA, 2003, p. 12.
[11] V.V. Nemoshkalenko, X-ray Photoelectron Spectroscopy of Metals and Alloys, Naukova dumka, Kiev, 1972.
[12] J. Jiang, A. Kucernak, Electrochim. Acta 47 (2002) 2381.
[13] R.N. Kyutt, E.A. Smorgonskaya, S.K. Gordeev, A.B. Grechinskaya, A.M. Danishevskiy, Fizika tverdogo tela 41 (1999) 1484.
[14] A.M. Suhotin, Handbook on Electrochemistry, Himiya, Leningrad, 1981.
[15] J.R. Scully, D.C. Silverman, M.W. Kending, Electrochemical Impedance: Analysis and Interpretation, STP 1188 ASTM ISBN 0-8031-1861-9.
[16] R. de Levie, Electrochim. Acta 8 (1963) 751.
[17] R. de Levie, Electrochim. Acta 9 (1964) 1231.
[18] I.D. Raistrick, Electrochim. Acta 35 (1990) 1579.
[19] K. Honda, M. Yoshimura, K. Kawakita, A. Fujishima, Y. Sakamoto, K. Yasui, N. Nishio, H. Masuda, J. Electrochem. Soc. 151 (2004) A532.
[20] K.P. Mishchenko, G.M. Poltoratskii, The Thermodynamics and Structure of Aqueous and Nonaqueous Solutions of Electrolytes, Himiya, Leningrad, 1976.
[21] J.V. Coe, Chem. Phys. Lett. 229 (1994) 161.
[22] M.D. Tissandier, K.A. Cowen, W.Y. Feng, J. Phys. Chem. A 102 (1998) 7787.
[23] Yu.Ya. Gurevich, Ju.B. Pleskov, Photoelectrochemistry of Semiconductors, Nauka, Moskva, 1983.
[24] B.E. Conway, Electrochemical Supercapacitors, Plenum Publishing, New York, 1999.